

## Flood Inundation Mapping using Microwave Remote Sensing and GIS Data Integration: A Case Study of Tungabhadra and Hagari River Subcatchments in North-East Karnataka, India

Lingadevaru D C, Govindaraju, Jayakumar P D, Somesha GS and Vinaya M  
*Department of Applied Geology, Kuvempu University, Shnakraghatta-577 451*  
*Corresponding Author: Lingadevaru D C*

**Abstract:** Floods become frequently occurring phenomena in the state of Karnataka, during the year 2009 there were torrential rainfalls over a short period of time due to the low atmospheric pressure in Bay of Bengal resulting vast areas flooded. The inundated extent analysis is of prime importance for mitigation of floods in this area. The traditional optical satellite images are not feasible for mapping the flooded area accurately due to bad weather condition, in this relevance the microwave remote sensing data offers an alternative solution to such limitations on account of its capability of penetration through clouds. In the present study Synthetic Aperture Radar (SAR) data of Radarsat-2, Quad polarimetric beam mode data has been used for mapping the extent of flood inundation. The processing of backscatter image is carried out using NEST application and threshold technique has applied to classify the water pockets using backscattered image in ERDAS environment. The GIS analysis and accuracy assessment has carried out using ArcGIS tools. The result shows around 10% of geographical area was inundated by flood and the most affected class in land use category is agricultural area which covers 1003.15 Km<sup>2</sup> and there are 178 settlements area affected drastically in Tungabhadra and Hagari river subcatchments.

**Keywords:-** Floods, Inundation, RADARSAT data, Backscatter Coefficient, Threshold, Visual Image Interpretation and GIS

Date of Submission: 21-01-2019 Date of acceptance: 05-02-2019

### I. INTRODUCTION

Flooding is mainly the result of extensive or continuous rainfall beyond absorptive capacity of the soil and flow capacity of streams and river channels, natural flow of a river is valuable and it is a natural and recurring event for any river or stream. In many parts of the globe, as abundant inhabitants is focused along the river valleys and flood is accountable for greater number of destructive events compare to any other natural hazards (Sultana, et.al, 2008). The major flood in more than 100 years has hits the most parts of the Karnataka and Andhra Pradesh States during 28th September to till 5th October 2009 belongs to south-east parts of India due to atmospheric depression in Bay of Bengal (Situation Report, 2009). In addition to heavy rains all the reservoirs built across the Krishna and Tungabhadra Rivers have been receives heavy inflows and their gates have been opened to discharge water downstream resulted flooding (IFRDRCS, 2009). Due to this, the large area remained as inundated for longer period resulted massive property damages, vast loss of agricultural crops and affected human beings. During the extreme flood incidence it is important to determine the rapid extent of flood inundation on land use land cover (Yong Wang et al, 2002).

The most important element for flood disaster management is availability of spatial maps and timely information for taking appropriate decisions and actions by the administrative authorities. The inundation maps derived based on remote sensing satellite images were extensively used for identifying the affected habitations, submerged roads and railways for carrying out rescue and relief operations (Bhat C.M, et.al., 2010). On other hand the selection of remote sensing imageries play important role for mapping the floods, because the optical remote sensing data being used for various applications related to earth resources studies and monitoring of the environment are very much successful. However these images are not feasible for all atmospheric weather conditions and which cannot capable to penetrate through clouds, mist and haze. In such circumstances microwave remote sensing is more suitable, the Synthetic aperture radar (SAR) data provides feasible way to acquire remotely sensed data through any atmospheric conditions for the specified time period. As the radar sensors are capable of acquiring earth features in all weather conditions, due to these unique features of radars their data makes it better choices for resources and disaster mapping in various applications (Vyjayanthi N, et. al., 2010). SAR radar system have fine azimuth resolution achieved by storing and processing of the data on

Doppler shift of multiple return pulses and the fine cross-track resolution obtained by the frequency modulation technique. This penetration capability offers a unique opportunity in using of radar data to map the floods (Yong Wang, 2002). Radar response is measured in terms of backscatter coefficient and it is dependent upon the sensor (polarization, frequency and looking angle) and the target parameters (surface roughness, dielectric constant and vegetation cover). In addition to this SAR being an active sensor, the data acquisition frequency is twofold increased with possibility of the data availability during both ascending and descending passes (Sesha Sai MVR, et al., 2010). Researchers found that visual image interpretation technique has most appropriate method to delineate the land and water boundaries but this become not appropriate in handling the water covers those were in close proximity with the paddy extents. The threshold technique is most appropriate method to extract inundation of flood and this has to been verified from DEM for relief and rescue operations (Sanjay K J, et. al., 2006).

This paper investigates the flood inundated areas by applying threshold classification technique using SAR data of RADARSAT-2, C-band quad polarimetric image. A threshold value is fixed for classifying water in the image by manually investigating the backscatter values in the flood pockets, river transects and lakes/ponds. The GIS processing is applied using Census/Administrative information to generate flood inundation and Damage assessment maps of Tungabhadra and Hagari river subcatchments of Karnataka.

## II. OBJECTIVES

- To extract flood inundated area map using RADARSAT data.
- To assess the damage extent of flood on Infrastructure and land use / land cover.

## III. STUDY AREA

The current study area belongs to north-east part of Karnataka in India. Agro-climatically the study area comes under semi-arid zone with dry climatic condition and lies between the 15° 00' 11.23" N to 16° 14' 34.60" N Latitude and 76° 18' 33.89" E to 77° 24' 5.85" E Longitude covers an geographical area of 12298.36Km<sup>2</sup> with large rural population and settlements. The study area starts from the mouth of Tungabhadra reservoir at west and drains up to the border of Karnataka state in Raichur district at east along the river Tungabhadra (Fig-1). It is located 1022 meters height from the mean sea level and has getting minimum temperature of 18.5 degree Celsius to maximum temperature of 45 degree Celsius with a normal rainfall of 806.8mm over the year (Report, 2010). The drainage pattern of study area is both highly dendritic and dendritic to sub dendritic in pattern. Geomorphologically it covers Flood plain, pediplain weathered, PIC and RH. Lithologically it covers granite, gneiss and Metabasalt. The soil covers fine, loamy, Clay and skeletal in nature (GSI District Resource Information).

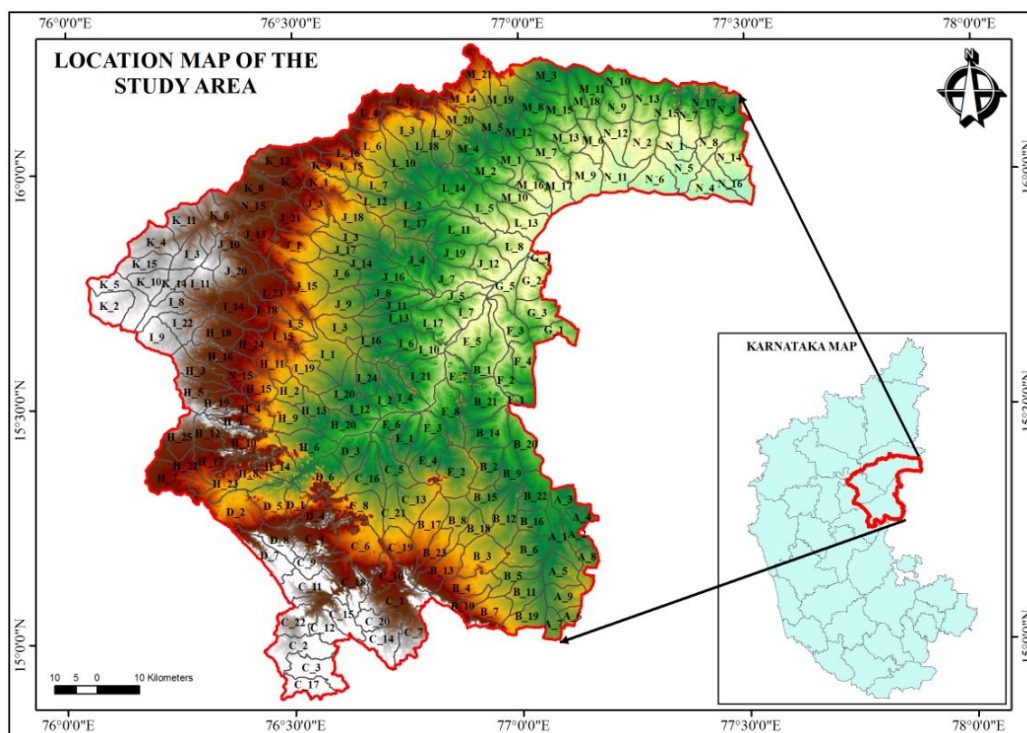


Figure 1: Location map of study area.

**IV. MATERIALS AND METHODOLOGY:**

The data utilized for study are, Survey of India toposheets (57 A, B, E and 56 D, H series) of 1:50,000 scale, Earth observation satellite images, rainfall data and ancillary data's such as Physiographic information, District/Taluk boundaries, Dept. of Agriculture (DoA) Crop statistics, Village/census data and relevant information from the concerned departments. The remote sensing images of multiple sensors and their image acquisition dates are shown in Table-1. Software's such as NEST and ERDAS Imagine are used for microwave SAR data processing and ERDAS Imagine is used for optical data processing. ArcGIS is used for preparation of various thematic layers and processing of GIS analysis. The accuracy assessment has been carried out based on ground truth points collected during the field work using handheld GPS instrument.

**Table 1:** Satellite data products and their acquisition dates.

<b>Remote Sensing Data</b>	<b>Sensor</b>	<b>Date of Acquisition</b>
Microwave SAR image	RADARSAT-2, C-Band(3.75-7.5 cm), Quad polarized (HH, HV, VV & HV) mode	6 <sup>th</sup> October 2009
Multi band Optical image	IRS P6 LISS-III (Before Flood)	(2&31) March 2009
	IRS P5 Awifs (During Flood)	4 October 2009
	IRS Resourcesat-2 LISS-IV	(Jan-March) 2011

The RADARSAT-2 is designed specifically to provide advanced SAR imaging capability by Canadian Space Agency, which operates at C-band (3.75 - 7.5 cm), frequency of 5.405 GHz with Quad Polarization (HH, VV, HV & VH) mode (Lori W, et.al, 2014). The image is imported in NEST 4B (Next ESA SAR Toolbox) SAR image processing software using product.xml information, the desired polarized layer (HH, HV and VV) to be displayed under R, G and B to generate FCC image view. Adjusted the Radiometric calibrations, terrain corrections (set to UTM WGS-1984, zone 43 projection) and speckle filtering (Lee, Median) were applied to generate the noise reduced image in Geotiff format. The values of pixel intensities are often transformed to a physical quantity called the backscattering coefficient or the normalization of radar cross-section, it is measured in decibel units (dB) with the values ranges from +5dB for very high brightest objects to - 40dB for very dark surfaces (Cunjian et.al, 1999). The formula for radar backscatter coefficient value in dB is shown below (Equation 1).

$$\text{Backscatter Coefficient} = 10 \text{ Log } (DN^2/A) + 10 \text{ Log } \text{Sin}(I) \quad \text{(Equation 1)}$$

Where; A is scale gain,  
I is angle of incidence and  
DN is Digital number recorded from image.

The process is carried out in NEST software. The threshold classification is applied to extract the water pixels in ERDAS imagine software, further GIS analysis has been carried out using ArcGIS tools.

For the multi-spectral optical imageries (IRS P6 LISS-III and R2 LISS-4), the image preprocessing has been carried out in ERDAS environment. The visual image interpretation technique is applied to generate the land use / land cover map up to level-3 classification using LISS-III satellite image of before flood (NRC-LU/LC-50K Project Manual, 2006). The base layers such as drainage networks and surface water bodies (Fig-3), transport networks and settlements (Fig-4) were generated using toposheets and updated using recent satellite imagery (IRS R2 LISS-IV image). Rainfall data analysis has been carried out, flood vulnerability map has been derived and damage extent on infrastructure and land use/land cover is assessed. GIS processing and accuracy assessment has been carried out using ground truth points (GTP) for all the layers. The fig-2 shows the step wise flow of work briefly.

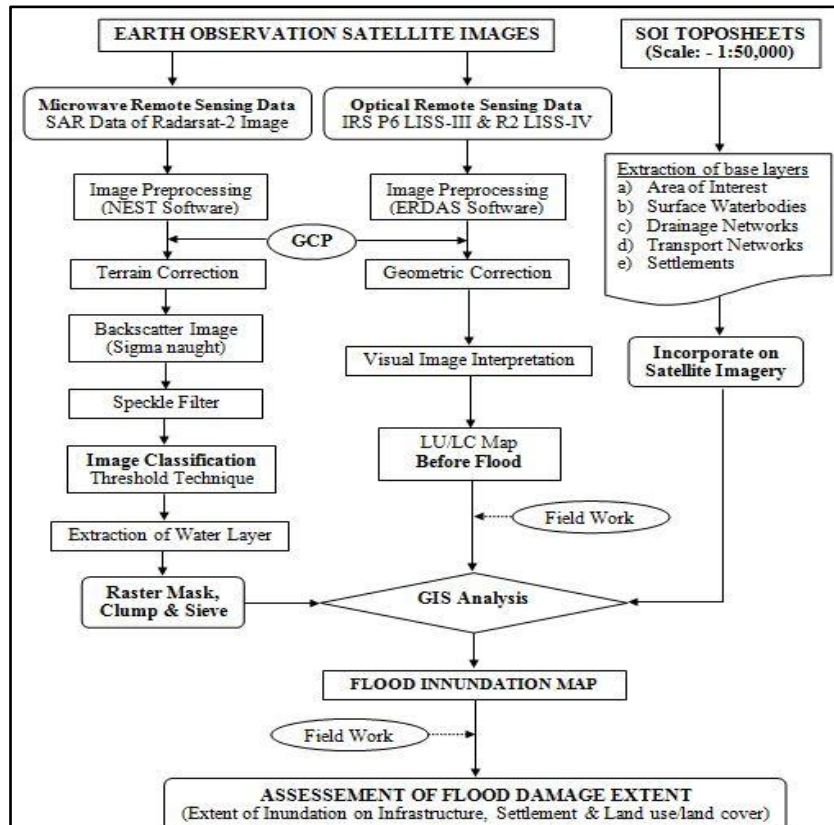


Figure 2:Flow chart showing brief methodology of the study.

## V. RESULTS AND DISCUSSIONS

### 5.1 SAR Analysis

Synthetic Aperture Radar (SAR) is well known for its ability to map the surface water. The determination of specific beam mode and polarization type to use when mapping the open water is dependent on the size of study extent and weather conditions. The present study area also covers comparatively bad weather condition during flood (Fig.-7). So we choose the quad polarimetric (HH, HV, VV & VH) beam mode data for the study of water body and water covered vegetation information. The processed backscatter (Sigma naught) and filtered (speckle reduced) image is applied for classifying the surface water information. The areas of smooth surfaces such as waterbodies are acts as a specular reflector, which results in the low backscatter pulse returns. It contrasts with rougher surface of the land, which diffuses the scatterer and produces the relatively higher amount of backscatters (Bhat C.M, et.al., 2010).

There are three different classification techniques were applied to generate the water pockets such as single threshold, segmentation and textural classification. It is observed that in segmentation and textural classification, over estimation and under estimation of water in some pockets is observed. In Single Threshold Classification the water area is better classified as compared to other techniques. In the present study, the single threshold technique is applied to select threshold values manually to extract the surface water information, which can be modified based on weather conditions, polarization and incidence angle of each individual scene. The HH polarization is often the best choice for mapping surface water because it is not as sensitive to small vertical differences in water caused by waves. HV polarization is preferable when high wind or surface roughness is present because there is significantly less effect on the backscatter compared to HH (Fig-8).

In HH polarization there is a complete distinction between the water and other objects surrounded on radar images with the backscatter values noticed. Water values are ranges from the minimum value of -40 dB for clear water to a higher value of around -12 dB, where the water has protruded by vegetation area with higher concentration of sediments. In current study, an attempt has made to derive the flood maps by choosing the various threshold values based on trial and error technique suggested by Gonzalez et.al, (2004). The ranges of threshold value from -12dB to -14dB were used to extract various flooding extent maps. The threshold model (The conditional statement for single threshold technique) may have to be run multiple times to achieve suitable results to fix the water pockets. The extracted water layer is masked using raster land use layer for removing the known surface waterbodies and canal commands. Refining is carried out for raster flood inundation layer using clump and sieve operations. The clump operation which classifies a continuous group of pixels in one class and

the sieve operation which filters very small clumps based on their size. Recoded the water layer to single bit (Fig-9) and converted the layer to vector format. The administrative boundaries up to village level, infrastructure (road and rail networks), settlements and land use land cover layers are overlaid for summarizing the flood inundated areas in ArcGIS environment. The result shows the extent of flood inundation in study area is 1043.09 Km<sup>2</sup>.

The accuracy assessment is determined for results of threshold technique using ground truth points (Waterbodies, flooded and non-flooded) collected at the time of during flood event and achieved the 82% of overall accuracy.

### 5.2 Extent of Flood Inundation on Infrastructure

The results shows 2.65 Km of railway track and 1247.51 Km of road networks including NH, SH, metalled, unmetalled, cart track and footpath were affected by flood inundation (Fig-12). There are 178 settlements are noticed under inundated areas which are directly affected and 501 villages are partially affected out of 1250 villages in the study area (Fig-11).

The overlay of drainage network and road network within the inundated area, it shows they may meet about 1940 places including major roads and railway tracks, which indicates that it is required to develop/reconstruct the cross drainage works (CD Works) at these places by making lot of focus on engineering (infrastructure) point of view.

### 5.3 Extent of Flood Inundation on Land use land cover

The land use land cover (LU/LC) layer is generated based on visual image interpretation and classification technique up to level-3 classification using IRS P6 LISS-III multi-spectral satellite image of before flood (Fig-5). The map reveals an area of 1.96 % of built-up, 5.45 % of forest, 82.21 % of agriculture, 7.43% of wasteland and 2.95 % of waterbodies area. In which 8.48 % of land surface (excluding 2.95% of surface waterbodies) is affected by flood inundation, the major category of land use class affected is agricultural land which covers an area of 1003.15 Km<sup>2</sup> under inundation (Fig-10). The various crops damaged due to floods are sugarcane, paddy, cotton, maize and chilly (as per the Dept. of Agriculture statistics). The details of land use classification and respective inundated area statistics is depicted in Table-2.

**Table 2:** The details of land use/land cover pattern and flood inundated area statistics.

Land Use / Land Cover Pattern		Mapped using Before Flood Imagery		Flood Inundated Area	
Level-1	Level-3	Area (Km <sup>2</sup> )	%	Area (Km <sup>2</sup> )	%
Built-Up	Built Up-Rural	114.58	0.93	14.97	0.12
	Built Up-Urban	57.04	0.46	2.44	0.02
	Built Up-Mining/Industrial area	69.51	0.57	4.04	0.03
Forest	Open	0.13	0.00	0.00	0.00
	Dense	6.17	0.05	0.00	0.00
	Scrub	627.76	5.10	0.51	0.00
	Plantation	1.67	0.01	0.00	0.00
	Tree Clade Area	34.67	0.28	0.11	0.00
Agriculture	Kharif Crop	2838.22	23.08	107.28	0.87
	Rabi Crop	1712.32	13.92	22.58	0.18
	Double Crop (Kharif+Rabi)	1659.02	13.49	217.86	1.77
	More than two crop	2214.75	18.01	629.60	5.12
	Plantation	19.70	0.16	0.87	0.01
	Current Fallow	1665.29	13.54	24.59	0.20
	Aquaculture / Pisciculture	0.70	0.01	0.37	0.00
Wasteland	Barren Rocky/Stony waste	240.36	1.95	4.67	0.04
	Open-Scrub	101.42	0.82	0.74	0.01
	Dense-Scrub	467.61	3.80	4.78	0.04
	Salt affected	98.46	0.80	7.60	0.06

Land Use / Land Cover Pattern		Mapped using Before Flood Imagery		Flood Inundated Area	
Level-1	Level-3	Area (Km <sup>2</sup> )	%	Area (Km <sup>2</sup> )	%
	Sandy area-Riverine	6.46	0.05	0.08	0.00
Waterbodies	River/Stream	281.54	2.29	0.00	0.00
	Reservoir/Tanks	28.39	0.23	0.00	0.00
	Lakes/Ponds	42.21	0.34	0.00	0.00
	Canal/Drain-Lined/Unlined	10.38	0.08	0.00	0.00
	<b>TOTAL</b>	<b>12298.36</b>	<b>100.00</b>	<b>1043.09</b>	<b>8.48</b>

### 5.4 Rainfall Distribution

The amount of runoff is related to the amount of rain a region experiences, 10 years annual average rainfall has been studied using inverse distance weighted (IWD) method. Analyzed the 45 rain gauge stations of the study area and the record show the annual average rainfall is varies from 363mm to 923mm. The intensity of rainfall distribution map is computed, the high rainfall trend shoes towards north-east portion and low rainfall trend shows towards southern portion of study area (Fig.6).

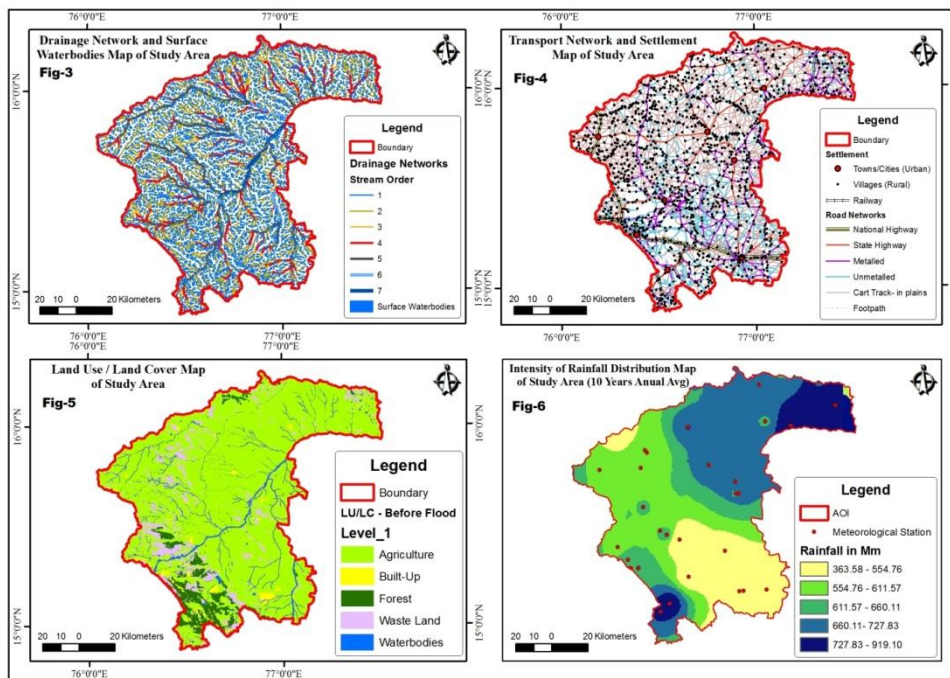


Figure: (3) Drainage network and surface waterbodies map, (4) Transportation & Settlement map, (5) Land use/land cover map, (6) Intensity of Rainfall distribution map

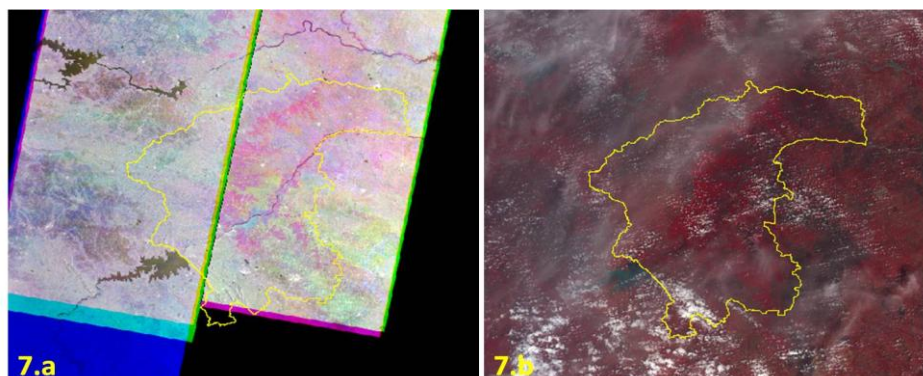


Figure 7: a) Microwave Remote Sensing data of Radarsat-2 FCC Image of 06/10/2009. b) Optical Remote Sensing data of IRS P5 Awifis Image of 04/10/2009.

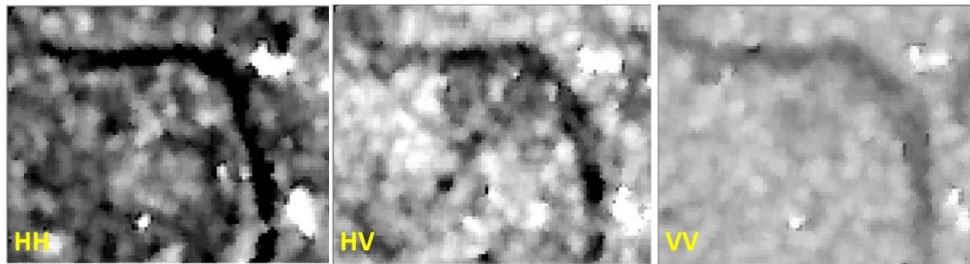


Figure 8: HH, HV and VV Channels over waterbody of Radarsat-2 image in study area.

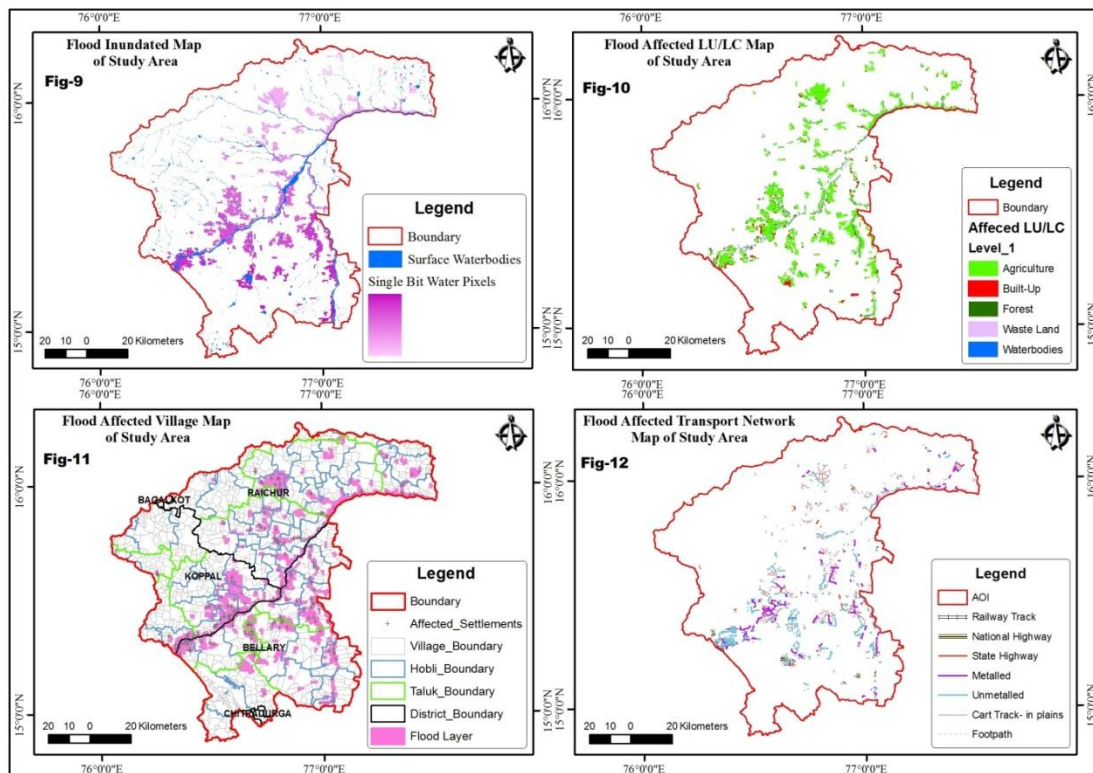


Figure: (9) Flood Inundation map, (10) Flood affected Land use / land cover map, (11) Flood affected Village map, (12) Flood affected Transport network map.

## VI. CONCLUSIONS

An amount of effort related to planning and management for mitigation of floods is mainly depends on the accurate information which is available about the disaster, its nature and extent in terms of time and space. In this study, an attempt has made to generate flood inundation area mapping using threshold classification technique on RADARSAT image. The results shows flood inundation map of the present study shows there are 178 settlements and 1057.66 Km<sup>2</sup> of area was affected. The flood inundated map is most useful to take appropriate measures and to handle the flood situation. Flooding cannot be prevented completely but it can be reduced or mitigated through the accurate information which is made available for planners about the severity and its large extent through maps. The remote sensing technology along with SAR data are known to be efficient and cost-effective for mapping and analyzing when large areas are affected by floods.

## VII. ACKNOWLEDGEMENTS

Authors would like to thank the Chairman and all senior faculty members for their support and to utilize the facilities in the Department of Applied Geology, Kuvempu University, JnanaSahyadri, Shankaraghatta-577 451. Also we would like to extend our special thanks to KRSAC, Bangalore, SAC, Ahmedabad and NRSC, Hyderabad for providing direct and indirect support.

## REFERENCES

- [1]. Bhat C.M, Rao G.S, Manjushree P, Bhanumurthy V, (2010). Space Based Disaster Management of 2008 Kosi Floods, North Bihar, India. *J. Indian Soc. Remote Sens.* 38, pp: 99-108

- [2]. Gonzalez, R.C., Woods, R.E and Eddians, S.L (2004), Digital Image processing using Matlab. *Prentice Hall, New Jersey*.
- [3]. GSI Map, Geological Survey of India - District Resource Information
- [4]. IFRDRCS (2009), India: Floods. International Federation of Red Cross and Red Crescent Societies. *Information bulletin no. 1, GLIDE no. FL-2009-000217-IND*.
- [5]. J. R. Jensen, *Remote sensing of the environment: an earth resource perspective* (Upper Saddle River, Prentice-Hall, 1996).
- [6]. T. M. Lillesand, R. W. Kiefer, and J. W. Chipman *Remote Sensing and Image Interpretation* (New York, John Wiley & Sons, Inc. 2004).
- [7]. Lori W, Brian B, Marilee P, Bill T and Lyle B (2014), Research Note: RADARSAT-2 Beam Mode Selection for Surface Water and Flooded Vegetation Mapping. *Canadian Journal of Remote Sensing*, 40, pp: 135–151.
- [8]. Natarajan A., Rajendra Hegde., Naidu L. G. K., Raizada A., Adhikari R. N., Patil S. L., Rajan K and Dipak Sarkar (2010), Soil and Plant Nutrient loss during the Recent Floods in north Karnataka: Implications and Ameliorative measures current science. 99(10).
- [9]. NRC LU/LC 50K Project Manual, (2011). National Land Use Land Cover Mapping using Multi-temporal Satellite Data. National Remote Sensing Centre, Dept. of Space, Govt. of India, Hyderabad - 500 625.
- [10]. Panigrahy S., Manjunath K.R., Chakraborty M., Kundu N. and Parihar J. S. (1999), Evaluation of RADARSAT Standard Beam data for identification of Potato and rice in India, *ISPRS Journal of Photogrammetry & Remote Sensing* 54, pp: 254-262.
- [11]. Report (2010), Biodiversity of Karnataka at a glance. [www.kbb.kar.nioc.in](http://www.kbb.kar.nioc.in)
- [12]. Sanjay K. J, Arun K.S, Ajanta G and Tanveer A (2006), Flood inundation mapping using NOAA AVHRR data. *Water Resource Management*, 20, pp: 949–959.
- [13]. MVR Sessa Sai, K. V. Ramana, and R. Hebbar, *Text book of Remote Sensing Applications* (NRSC / ISRO, Hyderabad, India. ISBN 978-81-909460-0-1, pp:14, 2010).
- [14]. Situation Report (2009), South India Floods-2009. *Sphere India: Unified Response Strategy*.
- [15]. Sultana, P., Thompson, P. and Green, C (2008), Can England Learn Lessons from Bangladesh in Introducing Participatory Floodplain Management? *Water Resource Management*, 22, pp: 357-376.
- [16]. Vyjayanthi N, Chdra S.J, and Raghavaswamy M (2010), Estimation of above ground biomass in Indian tropical forested area using multi frequency DLR-ESAR data, *Int. Journal of Geomatics and Geosciences* 1(2); pp: 167-178.
- [17]. Yong Wang, (2002). Mapping Extent of Floods: What We Have Learned and How We Can Do Better. *Nat. Hazards Rev.* 3, pp: 68-73.

IOSR Journal of Engineering (IOSRJEN) is UGC approved Journal with Sl. No. 3240, Journal no. 48995.

Lingadevaru D C. "Flood Inundation Mapping using Microwave Remote Sensing and GIS Data Integration: A Case Study of Tungabhadra and Hagari River Subcatchments in North-East Karnataka, India." *IOSR Journal of Engineering (IOSRJEN)*, vol. 09, no. 2, 2019, pp. 09-16.